

## Solution Dynamics and Stability of Lanthanide(III) (S)-2-(*p*-Nitrobenzyl)DOTA Complexes

Mark Woods,<sup>†</sup> Zoltan Kovacs,<sup>‡</sup> Robert Kiraly,<sup>§</sup> Ernő Brücher,<sup>§</sup> Shanrong Zhang,<sup>||</sup> and A. Dean Sherry<sup>\*,†,||</sup>

Department of Chemistry, University of Texas at Dallas, P.O. Box 830660, Richardson, Texas 75083, Macrocyclics, 2110 Research Row, Dallas, Texas 75235, Department of Inorganic and Analytical Chemistry, Lajos Kossuth University, H-4010, Debrecen, Hungary, and Rogers Magnetic Resonance Center, Department of Radiology, University of Texas Southwestern Medical Center, 5323 Harry Hines Boulevard, Dallas, Texas 75390

Received November 10, 2003

Addition of a benzyl substituent to the macrocyclic ring of DOTA has a substantial impact on the conformational ring flipping motion of the macrocycle in the resulting LnDOTA complexes. The *p*-NO<sub>2</sub>-benzyl substituent in the Ln(*p*-NO<sub>2</sub>-Bn-DOTA)<sup>−</sup> complexes lies in an equatorial position and effectively “locks” the conformation of the ring into the  $\delta\delta\delta\delta$  configuration. The presence of the *p*-NO<sub>2</sub>-benzyl group also increases the population of the square antiprismatic (SAP) coordination isomer for all Ln(*p*-NO<sub>2</sub>-Bn-DOTA)<sup>−</sup> complexes relative to that seen for the respective LnDOTA<sup>−</sup> complexes. Despite this increase in SAP isomer population, the rate of water exchange in these complexes remains comparatively fast. The kinetic and thermodynamic stabilities of the Ln(*p*-NO<sub>2</sub>-Bn-DOTA)<sup>−</sup> complexes are also slightly lower than the corresponding LnDOTA<sup>−</sup> complexes but appear to be sufficiently high for in vivo use.

### Introduction

Bifunctional chelates (BFCs) represent versatile building blocks in the search for new inorganic pharmaceuticals.<sup>1,2</sup> The ligating functionality of a BFC chelates the desired metal ion, and the second functionality, usually an electrophilic functional group, may be used to covalently attach the chelate to a biological targeting vector. This conjugation has wide-ranging appeal since it allows for radioisotopes to be conjugated to targeting vectors such as monoclonal antibodies for use in radioimmunotherapy,<sup>3,4</sup> for paramagnetic ions to be conjugated to targeting vectors that target and enhance the efficiency of MRI contrast agents,<sup>5,6</sup> and for Lewis acids to be conjugated to nucleic acid strands to act as artificial nucleases.<sup>7,8</sup>

Since the trivalent lanthanide and actinide ions have a wide variety of magnetic, fluorescence, and catalytic properties,<sup>9</sup> BFCs suitable for use with these ions are extremely useful. One such ligand, which has found widespread use, is (S)-2-(*iso*-thiocyanobenzyl)-DOTA (*p*-SCN-Bn-DOTA, Chart 1).<sup>1</sup> The lanthanide(III) complexes of the parent ligand DOTA have been widely studied,<sup>10–14</sup> but little has been published on the properties of either the complexes Ln(*p*-

\* To whom correspondence should be addressed. E-mail: sherry@utdallas.edu. Phone: +1 972 883 2907. Fax: +1 972 883 2925.

<sup>†</sup> University of Texas at Dallas.

<sup>‡</sup> Macrocyclics.

<sup>§</sup> Lajos Kossuth University.

<sup>||</sup> University of Texas Southwestern Medical Center.

(1) Woods, M.; Kovacs, Z.; Sherry, A. D. *J. Supramol. Chem.* **2002**, *2*, 1–15.

(2) Liu, S.; Edwards, D. S. *Bioconjugate Chem.* **2001**, *12*, 653–653.

(3) Kukis, D. L.; DeNardo, S. J.; DeNardo, G. L.; O'Donnell, R. T.; Meares, C. F. *J. Nucl. Med.* **1998**, *39*, 2105–2110.

(4) Li, M.; Meares, C. F.; Zhong, G. R.; Miers, L.; Xiong, C. Y.; Denardo, S. J. *Bioconjugate Chem.* **1994**, *5*, 101–104.

(5) De Leon, L.; Ortiz, A.; Weiner, A. L.; Zhang, S. R.; Kovacs, Z.; Kodadek, T.; Sherry, A. D. *J. Am. Chem. Soc.* **2002**, *124*, 3514–3515.

(6) Bhorade, R.; Weissleder, R.; Nakakoshi, T.; Moore, A.; Tung, C. H. *Bioconjugate Chem.* **2000**, *11*, 301–305.

(7) Huang, L. Y.; Chappell, L. L.; Iranzo, O.; Baker, B. F.; Morrow, J. R. *J. Biol. Inorg. Chem.* **2000**, *5*, 85–92.

(8) Hines, J. V.; Ammar, G. M.; Buss, J.; Schmalbrock, P. *Bioconjugate Chem.* **1999**, *10*, 155–158.

(9) Sigel, A.; Sigel, H. *The Lanthanides and Their Interrelations with Biosystems*; Dekker: New York, 2003; Vol. 40.

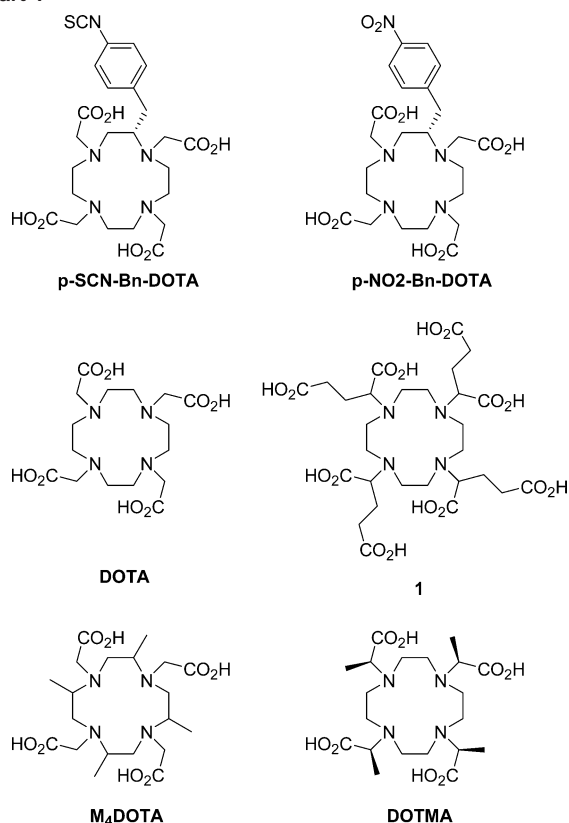
(10) Aime, S.; Barge, A.; Botta, M.; Fasano, M.; Ayala, J. D.; Bombieri, G. *Inorg. Chim. Acta* **1996**, *246*, 423–429.

(11) Hoefl, S.; Roth, K. *Chem. Ber.* **1993**, *126*, 869–873.

(12) Meyer, M.; Dahaoui-Gindrey, V.; Lecomte, C.; Guillard, L. *Coord. Chem. Rev.* **1998**, *180*, 1313–1405.

(13) Aime, S.; Botta, M.; Ermondi, G. *Inorg. Chem.* **1992**, *31*, 4291–4299.

Chart 1



SCN-Bn-DOTA)<sup>−</sup> or the precursor Ln(*p*-NO<sub>2</sub>-Bn-DOTA)<sup>−</sup> complexes. LnDOTA<sup>−</sup> complexes have very favorable kinetic and thermodynamic stabilities and are therefore often chosen as the basis of drugs for in vivo use. This is particularly important in situations where the complexes may be targeted to cells and not quickly excreted. Indeed, GdDOTA<sup>−</sup> has been widely used as an MRI contrast agent for many years, and other DOTA based systems are being developed.<sup>15</sup> Incorporation of an aryl *iso*-thiocyanate into the DOTA ligand facilitates conjugation of the chelate to a variety of targeting vectors using mild chemical conditions.

While the properties of the LnDOTA<sup>−</sup> complexes have been thoroughly examined, there have been few reports on the complexation properties of BFC analogues. Here, we report results of a study of the solution structures, stability, and properties of the lanthanide complexes of (*S*)-2-(*p*-nitrobenzyl)-DOTA (*p*-NO<sub>2</sub>-Bn-DOTA), the chemical precursor to *p*-SCN-Bn-DOTA.

## Experimental Section

**General.** (*S*)-2-(*p*-Nitrobenzyl)-DOTA was synthesized from L-phenylalanine using minor modifications of a procedure previously described.<sup>16,17</sup> The alkylation reaction to introduce the acetate pendant arms was performed with *tert*-butyl bromoacetate (MeCN/K<sub>2</sub>CO<sub>3</sub>/60 °C) rather than bromoacetic acid in water. The *tert*-butyl

esters were subsequently cleaved in aqueous hydrochloric acid, and the ligand was purified by precipitation from aqueous solution at pH 3 as the corresponding zwitterions. <sup>1</sup>H NMR spectra were recorded on a JEOL Eclipse 270 spectrometer operating at 270 MHz and a Varian Inova 500 spectrometer operating at 499.95 MHz. <sup>17</sup>O NMR spectra were recorded on a Varian Inova 500 spectrometer operating at 68.7 MHz. The 2D-EXSY spectrum was recorded at 500 MHz using 1024 × 1024 points, a mixing time of 40 ms was employed for the EXSY spectrum, and the COSY spectrum was recorded at 270 MHz using 1024 × 1024 points and a 90° pulse width of 7.5 μs. Variable temperature <sup>17</sup>O NMR spectra were recorded between 5 and 80 °C. Longitudinal relaxation times were measured using the inversion recovery method on a MRS-6 NMR analyzer from the Institut “Jožef Stefan”, Ljubljana, Slovenia, operating at 20 MHz. Relaxivity was determined by linear regression analysis of relaxation rates of six solutions (0.5–10 mM). Luminescence measurements were performed on a Perkin-Elmer LS50B fluorimeter.

**Thermodynamic Stability Constants.** Stock solutions of GdCl<sub>3</sub>, YCl<sub>3</sub>, and LuCl<sub>3</sub> were prepared by dissolving the lanthanide(III) oxides (Ln<sub>2</sub>O<sub>3</sub>) in 6 M HCl, and the excess acid was removed by evaporation at 60 °C. The concentration of LnCl<sub>3</sub> solutions was determined by complexometric titration, using EDTA and xylenol orange as an indicator. The concentration of *p*-NO<sub>2</sub>-Bn-DOTA solution was determined by pH–potentiometric titration, carried out in the presence and absence of excess CaCl<sub>2</sub>. The protonation constants of the ligand were calculated from the titration data obtained in the titration of 1.8 and 2.6 mM sample solutions with 100 mM Me<sub>4</sub>NOH in the pH range 1.7–12.2 (157 data points). The titrations were carried out with a PHM 93 Radiometer pH-meter, an ABU 80 autoburet, and a 6.0234.100 combined electrode (Metrohm) in a titration vessel thermostated at 25 °C. The titrated solutions (15 mL) were stirred with magnetic stirrer, and nitrogen was bubbled through the samples.

Due to slow formation of Ln(*p*-NO<sub>2</sub>-Bn-DOTA)<sup>−</sup> complexes, the stability constants were determined by the “out-of-cell” technique.<sup>18</sup> Nine separate samples (2.5 mL) were prepared in duplicate containing the ligand and GdCl<sub>3</sub>, YCl<sub>3</sub>, or LuCl<sub>3</sub>, each at 2.6 mM. Variable volumes of standardized 100 mM Me<sub>4</sub>NOH were added to each sample prior to sealing the samples under a blanket of N<sub>2</sub> gas to prevent entry of CO<sub>2</sub> during equilibration. Preliminary spectrophotometric studies with the Nd(III) complexes (570–590 nm) showed that equilibrium was reached in about 4 weeks. After this period of time, the potentiometric samples were opened, and the distribution of pH values in the samples was between pH 1.8 and 2.4. The proton concentration was calculated from the measured pH values using a correction term determined by titration of 10 mM HCl with 100 mM Me<sub>4</sub>NOH as a difference between the measured and calculated pH values.<sup>19</sup> All the equilibrium studies were made in 1.0 M Me<sub>4</sub>NCl solutions at 25 °C. The protonation constants ( $K_i^H$ ) and stability constants ( $K_{ML}$ ), defined as  $K_i^H = [H_iL]/[H_{i-1}L][H^+]$  ( $i = 1, 2, \dots, 6$ ) and  $K_{LnL} = [LnL]/[Ln^{3+}][L]$ , were evaluated from the potentiometric data using PSEQUAD.<sup>20</sup>

**Typical Procedure for the Preparation of Complexes for Spectroscopic Studies.** Eu<sub>2</sub>O<sub>3</sub> (1 equiv) and (*S*)-2-(*p*-nitrobenzyl)-DOTA (1 equiv) were mixed in water and stirred at 60 °C for 24

(14) Aime, S.; Botta, M.; Fasano, M.; Marques, M. P. M.; Geraldes, C. F. G. C.; Pubanz, D.; Merbach, A. E. *Inorg. Chem.* **1997**, *36*, 2059–2068.

(15) <http://www.probes.com/>.

(16) McMurry, T. J.; Brechbiel, M.; Kumar, K.; Gansow, O. A. *Bioconjugate Chem.* **1992**, *3*, 108–117.

(17) Renn, O.; Meares, C. F. *Bioconjugate Chem.* **1992**, *3*, 563–569.

(18) Burai, L.; Fabian, I.; Kiraly, R.; Szilagyi, E.; Brucher, E. *J. Chem. Soc., Dalton Trans.* **1998**, 243–248.

(19) Irving, H. M.; Miles, M. G.; Pettit, L. *Anal. Chim. Acta* **1967**, *28*, 475.

(20) Zékány, L.; Nagypál, I. In *Computational Methods for Determination of Formation Constants*; Leggett, D. J., Ed.; Kluwer: New York, 1985; p 291.

h. The reaction was filtered through 20  $\mu\text{m}$  syringe filter, and the solvent was removed by freeze-drying to yield the complex as a yellow solid in quantitative yield. The complexes were employed without further purification.  $[\text{Eu}(\text{NO}_2\text{BnDOTA})]^-$   $^1\text{H}$  NMR (270 MHz, D<sub>2</sub>O): major isomer only  $\delta = 34.8, 34.1, 31.4, 30.6, 9.5, 7.2$  (2H), 6.8 (2H), 5.2, 0.6, -1.0, -3.1, -3.8, -6.4 (2H), -7.1, -8.5, -9.8, -10.0, -10.6, -12.4, -13.7, -15.3 (2H), -15.7, 16.2 (2H), 16.9.  $m/z$  (ESI<sup>-</sup>): 686 (100% [<sup>151</sup>EuL]<sup>-</sup>), 688 (98% [<sup>153</sup>EuL]<sup>-</sup>).

## Results

**NMR Studies.** The structure and solution dynamics of the LnDOTA<sup>-</sup> complexes have been widely examined and are well understood. The macrocyclic ring adopts a square [3333] conformation with a carbon atom at each corner.<sup>12</sup> The four nitrogen donor atoms of the ring coordinate one face of the metal ion while the four oxygen atoms of the pendant arm carboxylates coordinate the opposite face. The coordination is completed by a capping water molecule.<sup>21</sup> The torsion angle between the coplanar nitrogen atoms and oxygen atoms then defines the coordination geometry of the ion. Two coordination geometries are adopted by LnDOTA<sup>-</sup>-like complexes, a capped square antiprism (SAP or M) (torsion angle  $\sim 39^\circ$ ), and a capped twisted square antiprism (TSAP or m) (torsion angle  $\sim 25^\circ$ ).<sup>12</sup> Since the conformation of the ring is associated with an element of helicity, the ring stereochemistry may be defined as either ( $\delta\delta\delta\delta$ ) or ( $\lambda\lambda\lambda\lambda$ ). The orientation of the arms is also associated with an element of helicity, defined as either  $\Delta$  or  $\Lambda$ . The coordination geometries may therefore be designated  $\Delta(\lambda\lambda\lambda\lambda)$  or  $\Lambda(\delta\delta\delta\delta)$  (SAP) and  $\Delta(\delta\delta\delta\delta)$  or  $\Lambda(\lambda\lambda\lambda\lambda)$  (TSAP). These four stereoisomers are related as two pairs of enantiomers. In solution these two coordination geometries are in dynamic equilibrium, the proportion of each being determined by the identity of the lanthanide ion and the ligand sidearms. Interconversion between the coordination geometries may occur by one of two processes, either ring flipping of the macrocyclic backbone carbons or rotation of the pendant arms. Sequential arm rotation and ring flips interconvert enantiomers (Figure 1).<sup>11</sup>

Since the rate of interconversion is slow on the NMR time scale ( $\sim 10\text{ s}^{-1}$ ),<sup>11</sup> the two coordination isomers are usually readily distinguished by  $^1\text{H}$  NMR spectroscopy. Two species are clearly visible in a ratio  $\sim 1:12$  in the extended spectral-width NMR spectrum of  $\text{Eu}(p\text{-NO}_2\text{-Bn-DOTA})^-$  (Figure 2). The spectrum of the major species (SAP) has been assigned by  $^1\text{H}$ - $^1\text{H}$  COSY NMR and by comparison with other related DOTA-type complexes.<sup>11,13,22</sup> The conformation of ethylene bridges in the macrocycle of LnDOTA<sup>-</sup> complexes is constrained into gauche conformation with a typical average N-C-C-N angle of  $59^\circ$ .<sup>23</sup> The sign of this angle (+ or -)

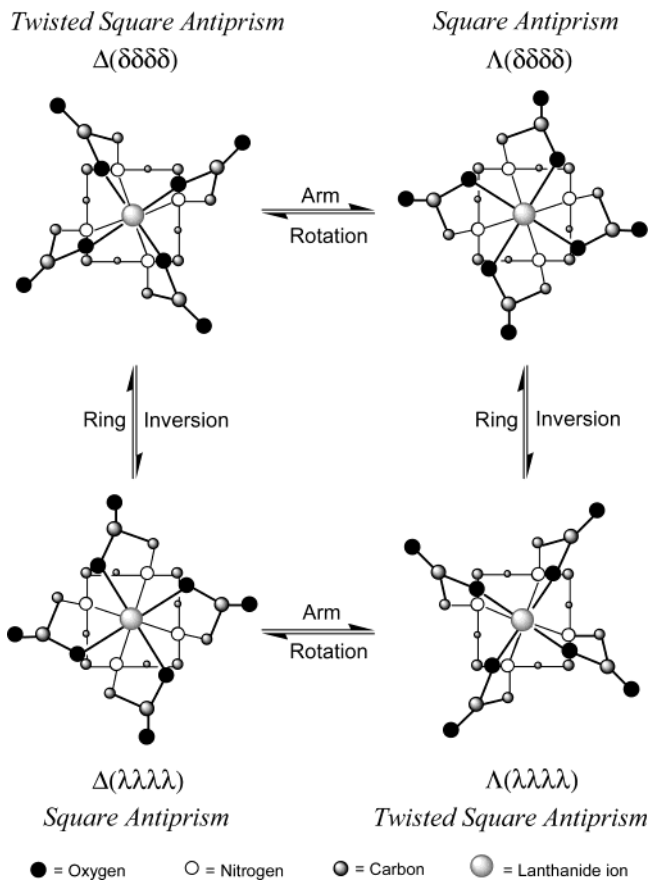


**Figure 1.** Interconversion pathways for the four stereoisomers of LnDOTA<sup>-</sup>.

defines the helicity of the ethylene bridge ( $\lambda\lambda\lambda\lambda$ ) or ( $\delta\delta\delta\delta$ ). This conformation minimizes both torsional and steric strain in the macrocycle providing an optimized binding conformation for the lanthanide ion. A gauche conformation places the four protons of the ethylene bridge into either one of two axial positions or one of two pseudoequatorial positions according to the Newman projection shown (Figure 2). As expected, the *p*-nitrobenzyl substituent was found to occupy a pseudoequatorial position on the macrocycle occupying the position of one H<sub>eq</sub>.<sup>24</sup> Interestingly, the nitrobenzyl group is located on the ethylene bridge with the smallest paramagnetic shifts of each proton; this is most noticeable in the case of H<sub>ax</sub>.<sup>24</sup> This is presumably the result of a distortion in the torsion angle of this ethylene bridge away from the perfect gauche conformation into a conformation in which the nitrobenzyl substituent lies in a more truly equatorial position (Figure 2). Although this must inevitably increase the torsional strain within this ethylene bridge, this gain in energy is probably offset by the decrease in steric strain gained by allowing the substituent to lie in this position. Examination of the chemical shifts of the most shifted axial protons of the ring allows assignment of the two species to their coordination geometries. The major species with the four axial proton resonances between 30 and 35 ppm corresponds to the more compact SAP geometry (M) while the four axial

(21) Dubost, J. P.; Leger, J. M.; Langlois, M. H.; Meyer, D.; Schaefer, M. *C. R. Acad. Sci., Ser. II: Mec., Phys., Chim., Sci. Terre Univers* **1991**, *312*, 349–354.

(22) Woods, M.; Aime, S.; Botta, M.; Howard, J. A. K.; Moloney, J. M.; Navet, M.; Parker, D.; Port, M.; Rousseaux, O. *J. Am. Chem. Soc.* **2000**, *122*, 9781–9792.

(23) Howard, J. A. K.; Kenwright, A. M.; Moloney, J. M.; Parker, D.; Port, M.; Navet, M.; Rousseaux, O.; Woods, M. *Chem. Commun.* **1998**, 1381–1382.

(24) Marques, M. P. M.; Geraldès, C. F. G. C.; Sherry, A. D.; Merbach, A. E.; Powell, H.; Pubanz, D.; Aime, S.; Botta, M. *J. Alloys Compd.* **1995**, *225*, 303–307.

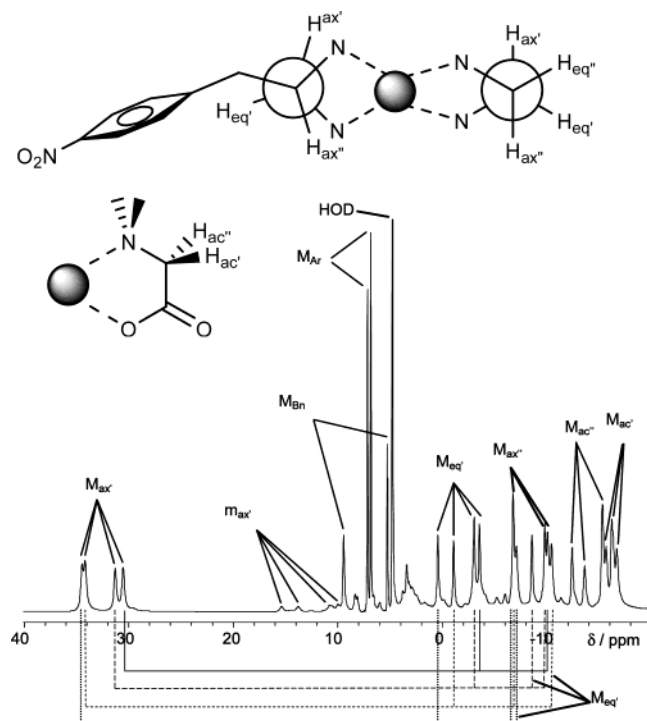


**Figure 2.** Extended spectral-width high-resolution  $^1\text{H}$  NMR spectrum of  $\text{Eu}(p\text{-NO}_2\text{-Bn-DOTA})^-$  recorded at pD 6, 25  $^\circ\text{C}$ , and 270 MHz. The spectrum of the major (SAP) isomer is assigned according to the labeling scheme shown. The lines underneath the spectrum indicate the couplings determined from the cross-peaks of the 2D COSY spectrum.

proton resonances between 10 and 15 ppm correspond to the more open TSAP geometry (m).<sup>22,25</sup>

For the  $\text{LnDOTA}^-$  complexes, the ratio of square antiprism (SAP) to twisted square antiprism (TSAP) depends on the ionic radius of the lanthanide ion.<sup>13</sup> Accordingly, the entire series of  $\text{Ln}(p\text{-NO}_2\text{-Bn-DOTA})^-$  complexes was prepared, and the ratio of the two dominant coordination isomers was measured by integration of the highly shifted axial proton peaks in their  $^1\text{H}$  NMR spectra (Figure 3). In common with the  $\text{LnDOTA}^-$  complexes, the TSAP isomer (m) is preferentially adopted in complexes formed by lanthanide ions with the largest ionic radii. As the ionic radius decreases from Ce to Tb, the proportion of the TSAP isomer steadily decreases. From Tb to Er, the complexes adopt almost solely the SAP (M) coordination geometry with only traces of the TSAP (m) isomer remaining. The population of the TSAP (m) isomer again increases for ions smaller than Er. This feature was also observed for  $\text{LnDOTA}^-$  complexes.<sup>14</sup>

Although the  $\text{LnDOTA}^-$  complexes exist as two enantiomeric pairs, placing a substituent on the macrocyclic backbone necessarily introduces a new chiral center rendering the enantiomeric complexes diastereomeric. In consequence, the four potential stereoisomeric forms of  $\text{Eu}(p\text{-NO}_2\text{-Bn-DOTA})^-$  [ $\Delta(\lambda\lambda\lambda\lambda)$ ,  $\Lambda(\delta\delta\delta\delta)$ ,  $\Delta(\delta\delta\delta\delta)$ , and  $\Lambda(\lambda\lambda\lambda\lambda)$ ] are diastereoisomers. The fact that only two species are visible in the  $^1\text{H}$  NMR spectrum suggests that two of these stereoisomeric forms have been rendered inaccessible by the

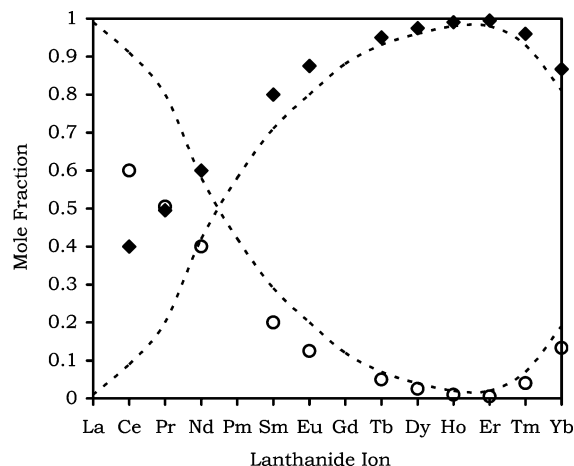


**Figure 3.** Fractions of the SAP (M) (◆) and TSAP (m) (○) coordination geometries for the  $\text{Ln}(p\text{-NO}_2\text{-Bn-DOTA})^-$  complexes as determined by  $^1\text{H}$  NMR at 25  $^\circ\text{C}$ . The dashed lines (---) represent the corresponding trend observed for  $\text{LnDOTA}^-$  complexes.

substitution of the macrocycle. This hypothesis is consistent with the observation of only two species for the acetate substituted DOTA derivatives  $\text{EuDOTMA}^-$ <sup>26,27</sup> and  $\text{Eu}(\text{RRRR-1})^-$ .<sup>22,23</sup> Substitution of the acetate arms effectively “freezes out” arm rotation locking the arms in one conformation.<sup>22,23,27</sup> The nature of the conformation ( $\Delta$  or  $\Lambda$ ) was determined by the configuration of the chiral center; an *S*-configuration conferring  $\Delta$  helicity on the arms, and an *R*-configuration,  $\Lambda$  helicity.<sup>22,23</sup> It was expected that the *p*-nitrobenzyl substituent was “freezing out” ring flip motion, and since the configuration at carbon was *S*, the macrocyclic ring would be locked into a ( $\delta\delta\delta\delta$ ) conformation.

Exchange spectroscopy (EXSY)<sup>11</sup> was used to probe the intramolecular dynamics of  $\text{Eu}(p\text{-NO}_2\text{-Bn-DOTA})^-$ . For each set of four resonances in the SAP (M) isomer, just one set of cross-peaks is observed in the EXSY spectrum (Figure 4). These peaks exchange with those of the TSAP (m) isomer, but only axial-to-axial and equatorial-to-equatorial exchanges were detected. This is consistent with isomer interconversions taking place only via arm rotation. No cross-peaks were observed corresponding to a ring flip motion, i.e., axial to equatorial. This is consistent with interchange between  $\Lambda(\delta\delta\delta\delta)$  and  $\Delta(\delta\delta\delta\delta)$  isomers, where  $\Lambda(\delta\delta\delta\delta)$  is the SAP (M) geometry, and  $\Delta(\delta\delta\delta\delta)$ , the TSAP (m) geometry (Figure 4). A similar observation of “frozen” ring motion was also reported for the tetramethyl substituted DOTA derivative,  $\text{M}_4\text{DOTA}$ .<sup>28,29</sup> Interestingly, this ring flipping motion was not inhibited when the DOTA backbone contained only one methyl group unlike that observed here for the *p*-nitrobenzyl substituent. It seems apparent therefore that the size of the substituent is critical in determining the extent of ring flipping motion in the macrocyclic ring.

(26) Brittain, H. G.; Desreux, J. F. *Inorg. Chem.* **1984**, *23*, 4459–4466.

(27) Di Bari, L.; Pintacuda, G.; Salvadori, P. *Eur. J. Inorg. Chem.* **2000**, 75–82.

(28) Ranganathan, R. S.; Raju, N.; Fan, H.; Zhang, X.; Tweedle, M. F.; Desreux, J. F.; Jacques, V. *Inorg. Chem.* **2002**, *41*, 6856–6866.

(29) Ranganathan, R. S.; Pillai, R. K.; Raju, N.; Fan, H.; Nguyen, H.; Tweedle, M. F.; Desreux, J. F.; Jacques, V. *Inorg. Chem.* **2002**, *41*, 6846–6855.

(25) Aime, S.; Barge, A.; Bruce, J. I.; Botta, M.; Howard, J. A. K.; Moloney, J. M.; Parker, D.; de Sousa, A. S.; Woods, M. *J. Am. Chem. Soc.* **1999**, *121*, 5762–5771.

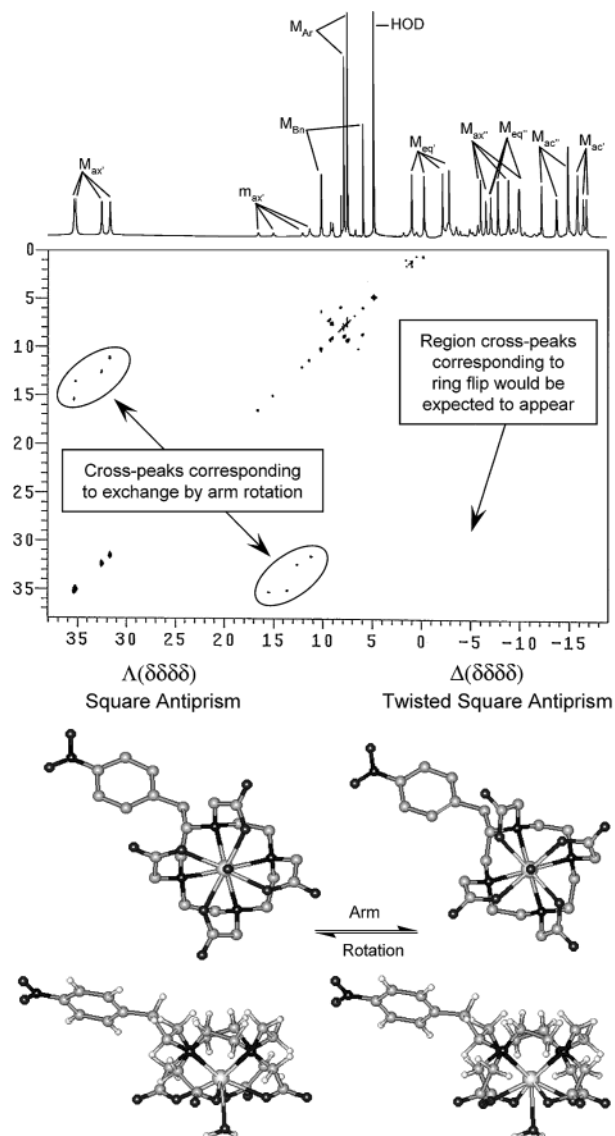


**Figure 4.** 2D <sup>1</sup>H EXSY spectrum of Eu(*p*-NO<sub>2</sub>-Bn-DOTA)<sup>-</sup> recorded at 25 °C, pD 6, and 500 MHz (top). As only two of the four possible diastereoisomeric coordination isomers are present (all four diastereoisomers are observed in the case of EuM-DOTA<sup>28</sup>), only one set of cross-peaks was expected for interconversion of these two diastereoisomers. The presence of cross-peaks corresponding to exchange of the axial protons of the SAP isomer ( $\delta = 30\text{--}36$  ppm) with the axial protons of the TSAP isomer ( $\delta = 11\text{--}17$  ppm) demonstrates that exchange occurs by arm rotation alone. The F2 axis is shown only as far as 0 ppm for the sake of clarity. Below the spectrum is a schematic representation of the  $\Lambda(\delta\delta\delta\delta)$  SAP (M) (left) and  $\Delta(\delta\delta\delta\delta)$  TSAP (m) (right) isomers showing their interconversion by arm rotation and the position of the *p*-nitrobenzyl substituent within the complex. The conformation and position of the *p*-nitrobenzyl substituent on the macrocycle is shown underneath.

The proportion of each coordination isomer present in solution may have a significant impact upon the application to which this BFC is applied. A number of recent studies have indicated that the two coordination isomers [SAP (M) and TSAP (m)] differ significantly in their properties.<sup>22,25,30</sup> These differences are likely to be most acute if the BFC is to be employed in an MRI contrast agent when optimization of water exchange is critical. The water exchange rate differs

by 1 order of magnitude between the two coordination isomers [SAP (M) and TSAP (m)]. The water exchange lifetime and isomeric ratio are therefore key factors when assessing the results of studies employing BFCs.

The hydration state of Eu(*p*-NO<sub>2</sub>-Bn-DOTA)<sup>-</sup> was measured using Horrock's method,<sup>31,32</sup> and when the corrections proposed by Parker and co-workers were taken into account, a value of  $q = 1.0$  was found.<sup>33</sup> The rate of water exchange in gadolinium complexes may be measured by fitting the line-widths of variable temperature <sup>17</sup>O NMR spectra of the solvent water (see ESI).<sup>34,35</sup> At 200 ns, the water residence lifetime ( $\tau_M$ ) of Gd(*p*-NO<sub>2</sub>-Bn-DOTA)<sup>-</sup> is comparable to that observed for GdDOTA<sup>-</sup> ( $\tau_M = 244$  ns).<sup>35</sup> The similarity in structure and water exchange rate between these two complexes no doubt accounts for similarity between the relaxivity of Gd(*p*-NO<sub>2</sub>-Bn-DOTA)<sup>-</sup> ( $r_1 = 4.7$  mM<sup>-1</sup>s<sup>-1</sup>) and GdDOTA<sup>-</sup> ( $r_1 = 4.2$  mM<sup>-1</sup>s<sup>-1</sup>)<sup>36</sup> at 20 MHz and 25 °C. From these observations, it may be surmised that the use of derivatives Gd(*p*-SCN-Bn-DOTA)<sup>-</sup> as the basis of MR contrast media accurately represents the effect of conjugation of a GdDOTA<sup>-</sup> complex. Nonetheless, it should be borne in mind that the  $\tau_M$  value at 200 ns is still somewhat short of the calculated optimal value of 25 ns required to achieve the highest water relaxivity.<sup>37</sup>

#### Kinetic and Thermodynamic Stability Determinations.

Owing to the toxicity of the lanthanide(III) ions, it is imperative that any complex used *in vivo* remains intact until the complex can be excreted. It is important then that the chelates formed by BFCs are both kinetically and thermodynamically stable. Given the parallels in complexation behavior between DOTA and *p*-NO<sub>2</sub>-Bn-DOTA, it was anticipated that the BFC forms complexes that have similar stability to the parent ligand. Under physiological conditions, no discernible dissociation of LnDOTA<sup>-</sup> complexes is observed before the complex is excreted.<sup>38</sup> Such slow dissociation renders measurement of the rate of dissociation impossible under such conditions. Acid mediated decomplexation is expected to be the primary mechanism for dissociation of anionic lanthanide complexes such as those of DOTA. Thus, challenging a complex with acid represents a reasonable measure of complex dissociation. Accordingly, 1 mM solutions of GdDOTA<sup>-</sup>, GdDOTMA<sup>-</sup>, and Gd(*p*-NO<sub>2</sub>-Bn-DOTA)<sup>-</sup> were incubated in nitric acid (pH 1), and the

(30) Dunand, F. A.; Aime, S.; Merbach, A. E. *J. Am. Chem. Soc.* **2000**, *122*, 1506–1512.

(31) Horrocks, W. D., Jr.; Sudnick, D. R. *J. Am. Chem. Soc.* **1979**, *101*, 334–340.  
 (32) Horrocks, W. D., Jr.; Sudnick, D. R. *Acc. Chem. Res.* **1981**, *14*, 384–392.  
 (33) Beeby, A.; Clarkson, I. M.; Dickins, R. S.; Faulkner, S.; Parker, D.; Royle, L.; de Sousa, A. S.; Williams, J. A. G.; Woods, M. *J. Chem. Soc., Perkin Trans. 2* **1999**, 493–504.  
 (34) Gonzalez, G.; Powell, D. H.; Tissieres, V.; Merbach, A. E. *J. Phys. Chem.* **1994**, *98*, 53–59.  
 (35) Powell, D. H.; Ni Dhubbghaill, O. M.; Pubanz, D.; Helm, L.; Lebedev, Y. S.; Schlaepfer, W.; Merbach, A. E. *J. Am. Chem. Soc.* **1996**, *118*, 9333–9346.  
 (36) Toth, E.; Pubanz, D.; Vauthey, S.; Helm, L.; Merbach, A. E. *Chem. Eur. J.* **1996**, *2*, 1607–1615.  
 (37) Aime, S.; Botta, M.; Fasano, M.; Terreno, E. *Chem. Soc. Rev.* **1998**, *27*, 19–29.  
 (38) Tweedle, M. F. In *Lanthanide Probes in Life, Chemical and Earth Sciences*; Bunzli, J. C. G., Choppin, G. R., Eds.; Elsevier: Amsterdam, 1989.

**Table 1.** Rates of Dissociation of  $\text{Gd}(p\text{-NO}_2\text{-Bn-DOTA})^-$ ,  $\text{GdDOTA}^-$ , and  $\text{GdDOTMA}^-$  in 0.1 M Nitric Acid

complex	$k_D$ (pH 1)/s <sup>-1</sup>
$\text{Gd}(p\text{-NO}_2\text{-Bn-DOTA})^-$	$6 \times 10^{-7}$
$\text{GdDOTA}^-$	$3 \times 10^{-7}$
$\text{GdDOTMA}^-$	$2 \times 10^{-8}$

**Table 2.** Protonation Constants of  $p\text{-NO}_2\text{-Bn-DOTA}^-$ <sup>a</sup>

equilibrium	log $K$ ( $p\text{-NO}_2\text{-Bn-DOTA}$ )	log $K$ (DOTA) <sup>b</sup>
$\text{L}^{4-} + \text{H}^+ \rightleftharpoons \text{LH}^{3-}$	10.93 (0.02)	12.6
$\text{LH}^{3-} + \text{H}^+ \rightleftharpoons \text{LH}_2^{2-}$	9.14 (0.03)	9.70
$\text{LH}_2^{2-} + \text{H}^+ \rightleftharpoons \text{LH}_3^-$	4.44 (0.04)	4.50
$\text{LH}_3^- + \text{H}^+ \rightleftharpoons \text{LH}_4$	4.19 (0.03)	4.14
$\text{LH}_4 + \text{H}^+ \rightleftharpoons \text{LH}_5^+$	2.33 (0.04)	2.32
$\text{LH}_5^+ + \text{H}^+ \rightleftharpoons \text{LH}_6^{2+}$	1.4 (0.05)	

<sup>a</sup> Values for DOTA are shown for comparison. <sup>b</sup> Measured in 0.1 M  $\text{Me}_4\text{NCl}$ .<sup>18</sup>

relaxivity was measured at periodic intervals. Dissociation of the complex results in an increase in the relaxivity as free gadolinium is released. Following the ratio of relaxivity over the initial relaxivity ( $\{r_1\}/\{r_1\}_0$ ) as a function of time allows the rate of dissociation under these conditions to be calculated.

The rates of dissociation of  $\text{Gd}(p\text{-NO}_2\text{-Bn-DOTA})^-$  and  $\text{GdDOTA}^-$  are comparable and slow, each taking several months to dissociate (Table 1). It is noteworthy that  $\text{Gd}(p\text{-NO}_2\text{-Bn-DOTA})^-$ , more conformationally restricted and therefore perhaps more rigid than  $\text{GdDOTA}^-$ , dissociates somewhat more quickly than the  $\text{GdDOTA}^-$ . In contrast, the rate of dissociation of  $\text{GdDOTMA}^-$  is an order of magnitude slower than that of the other two complexes. DOTMA is also more conformationally restricted than DOTA, but the difference appears to be the aspect of the complex which is rendered more rigid by substitution. Thus, it seems that for rigidity to affect the kinetic stability of a complex it must be applied to the part of the complex that will first be involved in the dissociative process. In this case that means the pendant arms. Thus, rigidification of the macrocycle backbone has a smaller effect upon the rate of complex dissociation since it is only involved late in the dissociative process.

The protonation constants of  $p\text{-NO}_2\text{-Bn-DOTA}$  are summarized in Table 2. For comparative purposes the values for the corresponding DOTA complexes are also shown. As can be seen, the first two protonation constants of  $p\text{-NO}_2\text{-Bn-DOTA}$  are lower than those of DOTA although the remaining constants are similar. The first two protonation constants of DOTA correspond to stepwise protonation of two diagonally opposing macrocyclic nitrogens while the next three constants correspond to protonation of carboxylates.<sup>39</sup> The fact that the protonation constants of the two most basic nitrogens are lower in  $p\text{-NO}_2\text{-Bn-DOTA}$  than in DOTA presumably reflects the conformational changes in the ethylene bridge of the macrocyclic ring induced by the  $p\text{-nitrobenzyl}$  substituent. This strain reduces the cooperative binding effect of the ligand, rendering these first two protons less tightly held thereby lowering the  $\text{p}K_a$ .

(39) Desreux, J. F.; Merciny, E.; Loncin, M. F. *Inorg. Chem.* **1981**, *20*, 987–991.

**Table 3.** Thermodynamic Stability Constants for Lanthanide Complexes of  $p\text{-NO}_2\text{-Bn-DOTA}^-$ <sup>a</sup>

equilibrium	$\text{Ln}(p\text{-NO}_2\text{-Bn-DOTA})^-$ log $K_{st}$	$\text{LnDOTA}^-$ log $K_{st}$
$\text{Gd}^{3+} + \text{L} \rightleftharpoons \text{Gd(L)}^-$	24.2 (0.03)	24.7 <sup>b</sup>
$\text{Y}^{3+} + \text{L} \rightleftharpoons \text{Y(L)}^-$	23.9 (0.04)	24.9 <sup>c</sup>
$\text{Lu}^{3+} + \text{L} \rightleftharpoons \text{Lu(L)}^-$	24.5 (0.05)	25.4 <sup>b</sup>

<sup>a</sup> Values for the corresponding DOTA complexes are shown for comparison. <sup>b</sup> Measured in 0.1 M  $\text{KCl}$ .<sup>41</sup> <sup>c</sup> Measured in 0.1 M  $\text{Me}_4\text{NCl}$ .<sup>42</sup>

The thermodynamic stability constants of the gadolinium, lutetium, and yttrium complexes of  $p\text{-NO}_2\text{-Bn-DOTA}$  were determined by potentiometric titration (Table 3). For comparative purposes the stability constants of the corresponding complexes of DOTA are also reported. As expected, the stability constants of the  $\text{Ln}(p\text{-NO}_2\text{-Bn-DOTA})^-$  complexes are very favorable but nevertheless slightly lower than those of the corresponding  $\text{LnDOTA}^-$  complexes. Thus, asymmetric substitution of the macrocyclic ring, which it had been concluded from our NMR studies distorts the gauche conformation of one of the ethylene bridges within the macrocycle, reduces the cooperative binding ability of the macrocycle. In consequence, the  $\text{p}K_a$  values of two of the nitrogens in the DOTA construct are lower than in DOTA, and this reduced basicity leads to a lower thermodynamic stability constant. This perturbation of the binding mode may lead to ever so slightly more rapid dissociation of the metal ion from the chelate as reflected in the kinetic stability studies. It has also been found that yttrium(III) complexes of nitrobenzyl substituted DTPA derivatives are about 1 order of magnitude less stable than the parent DTPA complex (log  $K_{ML} = 21.5$  vs 22.4 for YDTPA).<sup>40</sup> This may also be the result of changes in conformation around the substituted ethylene bridge. This hypothesis is supported by the observation that incorporating a cyclohexyl substituent onto the adjacent ethylene bridge, rigidifying the ethylene bridge into a gauche conformation, renders the corresponding complexes even more stable (log  $K_{ML} = 24.4$ ).<sup>40</sup> In comparison, the  $\text{Ln}(p\text{-NO}_2\text{-Bn-DOTA})^-$  complexes retain favorable thermodynamic stabilities, but more significantly they offer substantially improved kinetic inertness compared to BFC complexes derived from linear amines. Although it has been found that increasing the level of substitution in DTPA derivatives generally reduces that rate at which acid-catalyzed demetalation takes place, the rates of demetalation are still of the order of  $10^{-2}$  s<sup>-1</sup> in the best case.<sup>40</sup> This is a substantially more rapid than the rates of demetalation observed for  $p\text{-NO}_2\text{-Bn-DOTA}$  complexes and suggests that in vivo dissociation of the metal ion is likely to be higher when BFCs derived from linear amines are employed. Such favorable stability characteristics should offer a significant advantage for in vivo applications of  $\text{Ln}(p\text{-SCN-Bn-DOTA})^-$ -targeted complexes.

(40) McMurry, T. J.; Pippin, C. G.; Wu, C.; Deal, K. A.; Brechbiel, M. W.; Mirzadeh, S.; Gansow, O. A. *J. Med. Chem.* **1998**, *41*, 3546–3549.

(41) Cacheris, W. P.; Nickle, S. K.; Sherry, A. D. *Inorg. Chem.* **1987**, *26*, 958–960.

(42) Broan, C. J.; Cox, J. P. L.; Craig, A. S.; Katakay, R.; Parker, D.; Harrison, A.; Randall, A. M.; Ferguson, G. *J. Chem. Soc., Perkin Trans. 2* **1991**, 87–99.

## Conclusions

Substitution of a single benzylic substituent onto the macrocyclic ring of DOTA has a major influence on the ring flipping motion of the macrocyclic carbons in the corresponding lanthanide complexes. The conformation of the macrocyclic ring carbons ( $\delta\delta\delta\delta$  versus  $\lambda\lambda\lambda\lambda$ ) is determined by the stereochemical configuration at the carbon holding the substituent. Thus, a benzyl substituent derived from *S*-phenylalanine yields only the  $\Delta(\delta\delta\delta\delta)$  and  $\Lambda(\delta\delta\delta\delta)$  isomers in the corresponding  $\text{Ln}(p\text{-NO}_2\text{-Bn-DOTA})^-$  complexes. The added encumbrance of the benzyl substituent increases the proportion of the SAP (M) coordination isomer present in solution across the lanthanide series. Although this population difference is quite different from that seen for the corresponding  $\text{LnDOTA}^-$  complexes, this does not have a significant impact on the rate of water exchange as measured by  $^{17}\text{O}$  NMR. In consequence, the relaxivity of  $\text{Gd}(p\text{-NO}_2\text{-Bn-DOTA})^-$  is only marginally higher than that of  $\text{GdDOTA}^-$  at 20 MHz.

The diminished conformation mobility resulting from substitution of the macrocycle diminishes slightly the ability of the ligand to cooperatively bind metal ions. This results in slightly lower kinetic and thermodynamic stabilities for the lanthanide complexes of *p*-NO<sub>2</sub>-Bn-DOTA. In contrast, it appears that rigidifying the pendant arms decreases the

rate of complex dissociation by an order of magnitude. Nonetheless, with stability constants in excess of  $10^{23}$  and extremely slow dissociation kinetics, one would predict that the  $\text{Ln}(p\text{-NO}_2\text{-Bn-DOTA})^-$  complexes will be stable enough for in vivo applications. We have not taken equivalent measurements on the  $\text{Ln}(p\text{-SCN-Bn-DOTA})^-$  complexes, but it would be reasonable to assume that  $\text{Ln}(p\text{-SCN-Bn-DOTA})^-$  will have similar properties and hence conjugates of  $\text{Ln}(p\text{-SCN-Bn-DOTA})^-$  with various targeting vectors should be quite suitable for in vivo use over prolonged periods of time. Nonetheless, the bound water residence lifetime at 200 ns; although comparatively short, it is still substantially longer than is optimal (25 ns) for the design of high relaxivity MRI contrast media.

**Acknowledgment.** The authors thank the National Institutes of Health (RR-02584 and CA-84697), the Robert A. Welch Foundation (AT-584), and the Texas Advanced Technology Program for financial assistance.

**Supporting Information Available:** Additional figures and listings of the parameters used to fit the  $^{17}\text{O}$  variable temperature NMR. This material is available free of charge via the Internet at <http://pubs.acs.org>.

IC0353007